

^{31}P -CP–MAS NMR studies on TPP^+ bound to the ion-coupled multidrug transport protein EmrE

Clemens Glaubitz^{a,*}, Adriane Gröger^b, Kay Gottschalk^b, Paul Spooner^a, Anthony Watts^a, Shimon Schuldiner^c, Horst Kessler^{b,1}

^aDepartment of Biochemistry, Biomembrane Structure Unit, University of Oxford, South Parks Road, Oxford OX1 3QU, UK

^bDepartment of Organic Chemistry and Biochemistry, Technical University of Munich, Lichtenbergstrasse 4, D-85747 Garching, Germany

^cInstitute of Life Science, Hebrew University of Jerusalem, Jerusalem, Israel

Received 25 July 2000; accepted 25 July 2000

Edited by Thomas L. James

Abstract The binding of tetraphenylphosphonium (TPP^+) to EmrE, a membrane-bound, 110 residue *Escherichia coli* multidrug transport protein, has been observed by ^{31}P cross-polarisation–magic-angle spinning nuclear magnetic resonance spectroscopy (CP–MAS NMR). EmrE has been reconstituted into dimyristoyl phosphatidylcholine bilayers. CP–MAS could selectively distinguish binding of TPP^+ to EmrE in the fluid membrane. A population of bound ligand appears shifted 4 ppm to lower frequency compared to free ligand in solution, which suggests a rather direct and specific type of interaction of the ligand with the protein. This is also supported by the observed restricted motion of the bound ligand. The observation of another weakly bound substrate population arises from ligand binding to negatively charged residues in the protein loop regions. © 2000 Federation of European Biochemical Societies. Published by Elsevier Science B.V. All rights reserved.

Key words: EmrE; Tetraphenylphosphonium; Nuclear magnetic resonance spectroscopy; Magic-angle spinning; ^{31}P ; Multidrug resistance

1. Introduction

A sub-family of ion-coupled transporters, the small multidrug resistance (SMR) family (also called MiniTEXANS), seems to be rather suitable for structure–function studies due to their small size [1,2]. Members are between 107 and 115 residues of length and have been identified in *Staphylococcus aureus*, *Escherichia coli*, *Klebsiella aerogenes* and Gram-negative bacteria. The protein used in this study is the chromosomally encoded *E. coli* resistance protein EmrE [3]. Being one of the smallest ion-coupled transporters and due to its hydrophobic nature, EmrE has attracted much interest [3]. It has been shown that EmrE exchanges toxic cations such as methyl viologen, ethidium, acriflavin, tetraphenylphosphonium (TPP^+) and others in exchange for protons and is soluble in organic solvents. The protein can be functionally reconstituted into lipid membranes from organic solvent mixtures. A hydrophobicity analysis predicts a structure of four transmembrane helices as shown in Fig. 1a [4]. Transmission FTIR and oriented ATR-FTIR was used to determine

the secondary structure content and orientation of secondary structure elements in EmrE reconstituted in DMPC. A 80% helical contents was found. Amide H/D exchange experiments suggest a four-membered transmembrane helical bundle with an average helix tilt angle of 27° [5]. Liquid-state nuclear magnetic resonance (NMR) studies of EmrE in solvent mixtures support a four helical model of EmrE as well [6]. However, the length of individual helices are assigned slightly different compared to the hydrophobicity analysis. Especially helix I has been elongated by an amphiphilic helical link to helix II and the loop between helices 3 and 4 turned out to be longer (Fig. 1a). Negative dominance studies suggest that EmrE forms a functional trimer as judged by its reduced ability to transport while mixing active EmrE with non-active mutants [3,7]. Measurements of the accessibility of a series of 48 single Cys-replacements throughout the protein revealed a hydrophobic pathway for solutes in a tightly packed protein [8]. Binding studies of detergent solubilised EmrE support a homotrimeric model and show that Glu-14, the only membrane-buried charged residue, is required for substrate recognition [9]. Recently, two structural models of the trimeric transporter were presented. One was based on molecular dynamics using evolutionary conservation data [10] while the other was obtained by extensive MD calculations based on NMR-spectroscopic constraints [11].

A rather useful tool to obtain more specific information about substrate recognition, binding and transport is given by solid-state NMR since it allows to study the protein as close as possible to its native state in a lipid membrane [12–14]. The best probe of a binding site is the ligand itself. The effects produced by the transporter on the substrate are studied in a straightforward manner by observing the substrate in the presence of the transporter. It has been shown by Spooner et al., that observation of ^{13}C -labelled substrate in the binding site of the active galactose- H^+ symport protein GalP in its native environment, the inner membranes of *E. coli*, can be achieved by magic-angle spinning (MAS) NMR [15]. The experimental idea is to make use of the particular conditions for cross-polarisation (CP) to discriminate bound substrate alone. CP is a widely used technique in solid-state NMR to transfer magnetisation from abundant nuclei such as protons to rare nuclei such as ^{13}C in order to enhance their signal intensity [16]. This transfer usually takes place via dipolar couplings and is most efficient in rigid or frozen systems. Systems with different mobility should also have different CP characteristics, which allows to differentiate between highly mobile non-bound substrate and immobilised ligand bound

*Corresponding author. Fax: (44)-1865-275268/234.
E-mail: glaubitz@bioch.ox.ac.uk

¹ Also corresponding author. Fax: (49)-89-28913300/13210;
E-mail: kessler@ch.tum.de

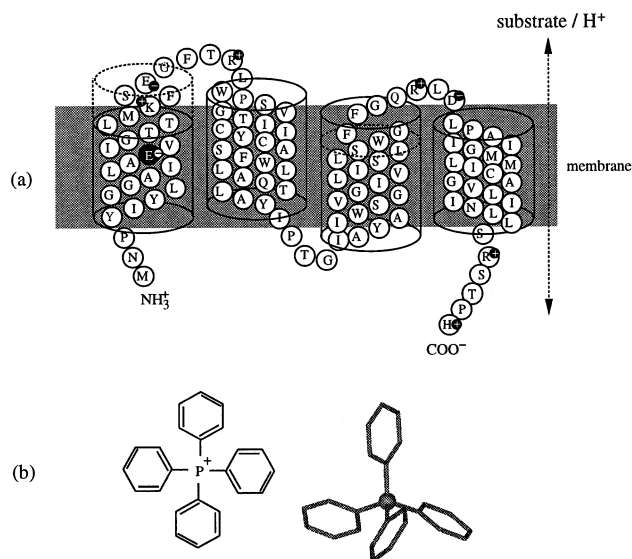


Fig. 1. Fold of EmrE protein predicted by hydropathy plots [3] and as analysed from liquid-state NMR data (dotted lines) [6] (a). Charged residues are labelled. EmrE is an *E. coli* multidrug transporter that removes a variety of toxins in exchange for hydrogen ions. The toxin used in this study is TPP⁺. TPP⁺ also binds to BmrR, a transcription activator of a multidrug transporter, whose crystal structure in the presence and absence of TPP⁺ is known [27]. The structure of TPP⁺ in the binding site is shown here (b).

to the membrane [15,17,18]. The theory of CP dynamics has been studied in detail in the past [19–21].

For the study presented here the high affinity substrate TPP⁺ ($K_D = 10$ nM [9], Fig. 1b) has been chosen in order to make use of some natural magnetic spin properties of the ³¹P nucleus such as 100% abundance, spin 1/2 and high sensitivity which makes it convenient to observe by NMR spectroscopy. In addition, it has other attractive features for studying transport mechanisms: the protein itself does not produce a background signal and there are normally only a limited number of ³¹P-containing moieties in the substrates giving rise to NMR signals which can be easily resolved and assigned.

2. Materials and methods

2.1. Protein overexpression, purification and reconstitution

Expression and purification of EmrE was done as described previously [4,6]. Reconstitution was achieved by making use of the solubility of EmrE in organic solvents. The protein was dissolved in chloroform:methanol (1:1) and a solution of L- α -DMPC (Sigma UK) in chloroform was added. After 30 min incubation the solution was dried under high vacuum for some hours and rehydrated in buffer (0.015 M Tris, 0.15 M NaCl, pH = 7.5). The molar protein to lipid ratio was 1:60 and 2.5 mg of protein were used. The proteoliposomes were pelleted, resuspended in buffer and layered on a linear sucrose gradient (0–50% w/w). Centrifugation (12 h, 4°C, 90 000 \times g) in a SW28 swinging bucket rotor (Beckman, USA) produced a layer at 25–28% w/w sucrose, indicating a homogeneously reconstituted sample (DMPC control at 17% w/w). The layer was recovered and the sucrose removed by several washing steps in buffer. The sample pellet was transferred into a 7 mm diameter zirconium MAS rotor.

To probe different protein:ligand ratios, small aliquots (3 μ l) of TPP⁺ bromide (TPP⁺) from a 0.07 M stock solution (Aldrich) were added stepwise to the sample in the MAS rotor. NMR experiments were carried out after a 30 min incubation time at 30°C after each titration step. During incubation the sample was set spinning to ensure an even distribution and good mixing of sample and ligand.

2.2. NMR experiments

All NMR experiments were performed at 161.3 MHz for ³¹P and 400.13 MHz for ¹H on a Bruker DMX-400 spectrometer using a Bruker 7 mm double resonance MAS probe. A proton field strength of 55 kHz was applied for CP and proton decoupling. The field strength applied to ³¹P spins was adjusted to satisfy the Hartmann–Hahn condition for CP from protons in the sample. The same power levels were used for making observations by direct ³¹P irradiation. The CP contact time was varied between 0.1 and 5.0 ms. A repetition delay time of 2.0 s was applied. A spinning rate of 2500 Hz was used throughout this study and controlled to within ± 5 Hz. Observations were made in both the L _{α} (liquid crystalline) and L _{β} (gel) phase at 30°C and 7°C respectively. The temperature was regulated by a Bruker BT3000 temperature control unit. Spectra were analysed using Felix (Biosym).

3. Results

The proton-decoupled ³¹P-MAS spectrum recorded from DMPC vesicles (19.2 μ mol, 13 mg) containing 1 μ mol TPP⁺ is shown in Fig. 2a. The spinning speed was set to 2500 Hz, which is less than the DMPC ³¹P chemical shift anisotropy and causes spinning sidebands equally separated from the isotropic chemical shift. The TPP⁺ resonance is observed at 23.2 ppm, consistent with the literature value [22], between sidebands +1 and +2.

Different from established applications to rigid systems, CP-MAS is used here not for signal enhancement but merely as a ‘dynamic filter’ to observe substrate immobilised by binding to the membrane. In order to achieve this, the membrane has to remain in the fluid state (above 273 K). CP should then be incapable of detecting non-associated substrate due to the motional averaging of dipolar coupling in solution [15]. The CP-MAS spectrum in Fig. 2b does not contain any signal from TPP⁺. CP fails to detect the substrate, which means TPP⁺ is not immobile in the fluid DMPC membrane and undergoes isotropic tumbling instead.

Fig. 2c shows a proton-decoupled ³¹P-MAS spectrum of DMPC proteoliposomes containing 0.2 μ mol EmrE (2.5 mg) at a lipid:protein ratio of 60:1 with 0.5 μ mol TPP⁺. In contrast to the spectrum in Fig. 2b, CP reveals two signals of different intensities at frequencies of 22.9 ppm (TPP-1) and 19.0 ppm (TPP-2) (Fig. 2d). Since the substrate can be observed by CP it must be immobilised on the relevant NMR time-scales (ms), which can best be explained by binding to the protein. Both observed TPP⁺ chemical shifts changed by -0.3 ppm (TPP-1) and -4.2 ppm (TPP-2) compared to the substrate in solution. Especially the shift for TPP-2 is of significant size and points toward a direct interaction between ligand and protein.

The membrane dynamics can be probed qualitatively by studying CP build-up curves for different membrane components as shown in Fig. 3. Lipids are highly mobile. Their dynamics in a liquid-crystalline membrane is characterised by internal motions (*trans-gauche* isomerisation, $\tau_i \sim 10^{-11}$ s), intermolecular motions (rotational diffusion about long axis $\tau_{R||} \sim 10^{-10}$ s, and wobbling of long axis $\tau_{R\perp} \sim 10^{-9}$ s) and collective motions where the whole membrane undergoes undulations (10^{-3} – 10^{-6} s) [23,24]. Therefore, ¹H–³¹P dipolar couplings are reduced and CP is rather inefficient. A long contact time of 5 ms is needed to reach an optimum signal intensity as shown in Fig. 3b after which the intensity slowly decays. The observed fluctuations within the first 0.5–1 ms are typical for CP build-up curves of dynamic molecules such as

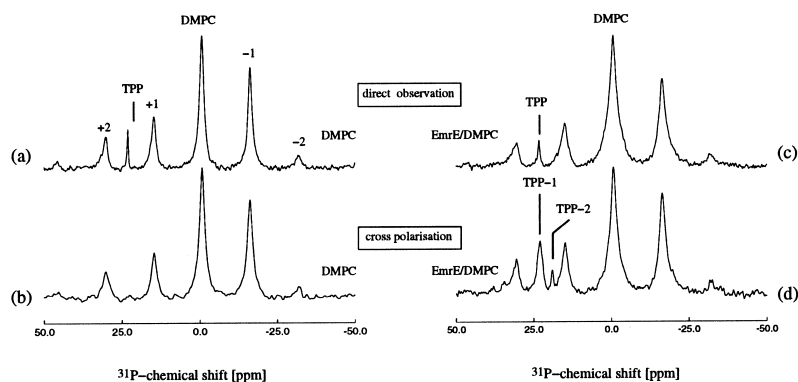


Fig. 2. ^{31}P -MAS spectrum under ^1H decoupling of DMPC with added TPP $^+$ (DMPC:TPP $^+$ = 20:1 mol/mol) (a). The isotropic lines are labelled with TPP $^+$ (23.2 ppm) and DMPC (−0.7 ppm). The indices −2, −1, +1, +2 denote DMPC spinning sidebands. Under ^1H - ^{31}P CP (here shown for 0.6 ms contact time), no TPP $^+$ could be detected in the DMPC sample (b). The proton decoupled ^{31}P -MAS spectrum of DMPC vesicles containing 0.2 μmol EmrE (2.5 mg) at a lipid:protein ratio of 60:1 with 0.5 μmol TPP $^+$ (c) shows no significant difference to spectrum (a), but under CP two additional resonances (1 = 22.9 ppm, 2 = 19.0 ppm) appear (d). All spectra were acquired at 161.3 MHz for ^{31}P , $T = 280$ K and sample rotation rate $\omega_r = 2500$ Hz. The chemical shift is referenced with respect to H_3PO_4 (85% solution).

lipids in a fluid membrane. The build-up of bound TPP however is more rapid and reaches its optimum already at 1.6 ms for TPP-1 and at 0.5 ms for TPP-2. This indicates, that TPP $^+$ while bound to EmrE is substantially less mobile than DMPC. In addition, it can be concluded that the component TPP-2 is less mobile than TPP-1.

The molar ratio of TPP $^+$:EmrE used here was 2.5:1. Additional experiments at different ligand:protein ratios were performed. For sub-stoichiometric quantities (0.3 mol/mol) only one signal, TPP-1, could be observed. Its intensity did increase by adding more substrate to the sample pellet. In contrast however, TPP-2 appeared for TPP $^+$:EmrE > 2 mol/mol and remained almost unchanged by adding more ligand.

4. Discussion

Our CP results demonstrate that the substrate transporter complex exists for a lifetime, that is long on the experimental time scale (ms). This is consistent with the known high-affinity binding of TPP $^+$ to EmrE ($K_D = 10$ nM) [9].

The most interesting result is the appearance of a TPP $^+$ signal shifted by −4.2 ppm with respect to free substrate in solution. Chemical shifts measured in ^{31}P NMR are related to shielding by the electron cloud around the phosphorus nucleus. Factors that influence the distribution of these electrons are expected to lead to changes in the chemical shift. These factors could be conformational changes of the molecule or changes in its environment. Although changes in charge should not necessarily lead to changes in the chemical shift [25], they can be accompanied by more relevant parameters such as bond geometry, electronegativity of substituents and the relative amounts of π -bindings. Another contribution is ring-current shifts caused by binding of the phosphoryl moiety in the vicinity of an aromatic residue. These conditions are fulfilled if the ligand would interact specifically with the protein, causing dramatic changes in its environment and also likely to enforce some changes in its average conformation. It has been shown by scanning the cysteine accessibility of EmrE, that the protein is rather tightly packed without any continuous aqueous domain but with a hydrophobic pathway for solutes [8]. This would indeed be required for a substrate

like TPP $^+$ to interact directly with the protein causing changes of the existing protein and substrate structure. In addition, it has been found, that the membrane-embedded charged residue Glu-14 is required for ligand binding [9]. Interestingly, TPP $^+$ also interacts specifically with BmrR, a transcription activator of the gene for the *Bacillus subtilis* multidrug transporter Bmr [26]. There, TPP $^+$ binding is mediated by van der Waals contacts with multiple hydrophobic residues in the pocket but mainly by an electrostatic interaction between the positively charged substrate and Glu-134 at the bottom of the binding site [27]. The structure of TPP $^+$ while bound to BmrR is shown in Fig. 1b. The tetrahedral symmetry of the phosphonium ion TPP $^+$ requires all bond angles to be 109.5°. However, the structure of the bound substrate is distorted and all bond angles between the phenyl rings and the phosphorus nucleus deviate between 1 and 5° from symmetry. It is not unreasonable to assume, that similar structural changes would occur for TPP $^+$, strongly bound to tightly packed EmrE, in order to explain the relatively large chemical shift difference of −4.2 ppm. A number of studies suggest that bond angle distortion effects are most important in order to explain ^{31}P chemical shift differences although they are also inseparably intermixed with electronegativity and π -electron overlap effects [28]. In our case, phenyl can act as a π -electron donor to the empty 3d orbitals of phosphorus in the phosphonium compounds and so conformational changes would contribute here as well to these effects. ^{31}P chemical shift changes of phosphate moieties in substrates and inhibitors so far measured in complexation with enzymes are usually less than 2 ppm, but changes of 4–5 ppm have been detected [29]. The largest enzyme-associated ^{31}P perturbation is the observation that the phosphate covalently bound to alkaline phosphatase is shifted 6–8 ppm down-field from inorganic phosphate in solution [30–32]. It has been suggested that a shift in the pK of the phosphate as well as bond-angle strain in the enzyme complex account for this effect [31]. The precise conformation of TPP $^+$ bound to EmrE cannot be derived just based on chemical shift changes, but it can be concluded that TPP-2 is actually the substrate strongly bound in the binding pocket.

It is now necessary to explain origin and potential meaning

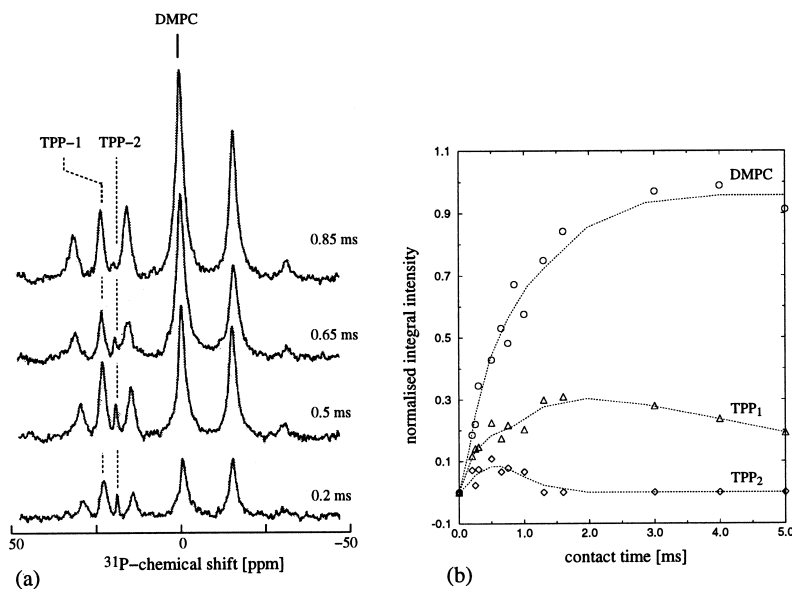


Fig. 3. ^{31}P -CP MAS spectra of EmrE/DMPC (1:60) containing TPP^+ at different contact times (a). The CP profile for the isotropic DMPC signal and both observed TPP^+ resonances reveals that the best polarisation transfer for the lipid takes place at longer contact times, while the optimum for TPP_1 is observed at 1.6 ms and for TPP_2 at 0.5 ms. The dotted lines are of no theoretical significance.

of the other observed bound TPP^+ population (TPP_1). Its chemical shift changes only by -0.3 ppm. This means, that only small structural and/or environmental changes occur. As concluded from our control experiments (Fig. 2a,b), no non-specific binding to the lipids is detected. Therefore, it must also bind to the protein. However, TPP_1 is motionally less restricted than TPP_2 in the binding pocket judging from the CP build-up curves. A possible explanation is that low-affinity, non-specific binding to charged residues in the hydrophilic loop regions takes place. EmrE contains five cationic residues (Lys-22, Arg-29, Arg-82, Arg-106, His-110) and three carboxylates (Glu-14, Glu-25, Asp-84) as shown in Fig. 1a. Only Glu-14 is predicted to be membrane-embedded whilst all other residues are expected to be accessible from the solvent. It is therefore feasible that TPP^+ binds via electrostatic interactions to the negatively charged residues Glu-25 and Asp-84. This binding would not cause essential chemical shift changes and TPP^+ would be motionally less restricted since it is not bound into a tight binding pocket. The question of course is, whether this additional substrate binding is actually required for transport or whether it is a less important side-effect. It is interesting to note, that the signal intensity of TPP_1 did increase with titrating substrate into the sample pellet but TPP_2 just appeared from $\text{TPP}^+:\text{EmrE} > 2$ mol/mol and remained almost unchanged which hints toward a functional mechanism. The crystal structure of transcription factor BmrR with and without bound TPP^+ reveals a drug-induced unfolding and relocation of an α helix, which exposes an internal drug-binding pocket. It has been argued that the ligand TPP^+ induces these structural changes by interactions with charged residues [27]. A similar cooperative process could take place here. In that case, EmrE would be oriented in the membrane with both N- and C-terminal pointing into extracellular space, while the carboxylates Glu-25 and Asp-84 on the opposite side are required to interact with the substrate prior its translocation out of the cell (Fig. 1a). This assumption is supported by a recent computational model of EmrE representing a

closed form of the ion coupled transporter [11]. The negative charge of the central Glu-14 is exposed to the same side as Glu-25 and Asp-84, indicating that this side may indeed be intracellular. The charge distributions of the putatively intracellular side is shown in Fig. 4. The proximity of the residues Glu-25 and Asp-84 in this model suggest that the ligands are attracted by these residues, constituting a weak binding site. Weak binding to these positions might lead to an unfolding of a short amphiphilic helix which connects helix I and II in the model. This helix is part of a lid that closes the intracellular side of the protein, partially shielding Glu-14. Such an helix

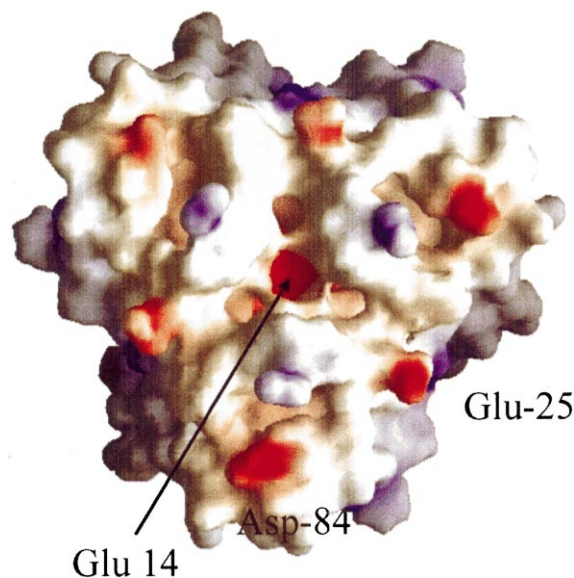


Fig. 4. Simulated charge distribution of EmrE viewed from putatively intracellular side (for details see [11]). The negatively charged residues Glu-25 and Asp-84 are located on the protein surface allowing weak binding of TPP^+ . Strong binding is mediated by Glu-14 buried inside the hydrophobic core of EmrE.

unfolding event would compare to the structural changes observed in BmrR.

Replacing each one of the carboxyl residues Glu-25 and Asp-84 in the loops with Cys has no effect on the activity of the transporter. Replacement of both carboxylates, however confers decreased resistance in vivo and shows only marginal transport activity in proteoliposomes [33]. In contrast, TPP binding to the double mutant takes place with nearly the same affinity as to the wild type [34], which points toward a more indirect or even no involvement of the carboxylates in substrate recognition. Further biochemical as well as NMR investigations are required in order to understand the role of Glu-25 and Asp-84 better.

It shall be pointed out, that our observations here do not contradict previous biochemical studies. Binding studies of observed $^3\text{H-TPP}^+$ to detergent solubilised EmrE- His suggested 0.25–0.3 mol of TPP^+ per mol of EmrE bound with a K_D of 10 nmol [9]. Detergent effects could alter the possibility of weak substrate binding to the protein surface so that only substrate in the binding pocket is detected. In addition low affinity binding might be difficult to detect with radioactive ligands.

It is not trivial to analyse the stoichiometry in the presented study, since the precise correlation between observed CP intensities for DMPC, TPP-1, TPP-2 and their concentration depends on a number of factors such as dynamics and CP contact time. It is however save to conclude that the molar quantity of substrate contributing to TPP-1 is actually larger than the strongly bound population of TPP-2 (Fig. 3). Assuming the same CP efficiency for both TPP-1 and TPP-2, their intensity ratio can be interpreted as molar ratio of between 4:1 and 6:1. This observations would be consistent with the recently presented computational model of EmrE [11]. The surface-exposed negatively charged residues Glu-25 and Asp-84 would allow weak binding to more molecules than Glu-14 which is buried in a tight hydrophobic pore in the centre of the trimer, mediating strong substrate binding (Fig. 4).

5. Conclusions

In this study, the cationic lipophilic substrate TPP^+ has been observed bound to EmrE by $^{31}\text{P-CP-MAS}$ NMR spectroscopy. The large chemical shift difference of -4.2 ppm and the observed CP build-up profile suggest a rather specific and direct interaction of the ligand with the protein. The observation of another weakly bound substrate population is interpreted as ligand binding to negatively charged residues in the protein loop regions.

The results demonstrate a rather promising approach to study multi-drug transport systems close to their native state and encourage more detailed solid-state NMR studies in combination with isotope labelling towards an understanding of substrate binding and transport.

Acknowledgements: This work was supported by the German–Israeli Project Cooperation on Future-oriented Topics (DIP) and Deutsche Forschungsgemeinschaft (Emmy Noether-Research Fellowship for C.G.).

References

- [1] Grinius, L., Dreguniene, G., Goldberg, E.B., Llia, C.H. and Projan, S.J. (1992) *Plasmid* 27, 119–129.
- [2] Paulsen, L.T., Skurray, R.A., Tam, R., Saier, M.H., Turner, R.J., Weiner, H., Goldberg, E.B. and Grinius, J.L. (1996) *Mol. Microbiol.* 19, 1167–1175.
- [3] Schuldiner, S., Lebendiker, M. and Yerushalmi, H. (1997) *J. Exp. Biol.* 200, 335–341.
- [4] Yerushalmi, H., Lebendiker, M. and Schuldiner, S. (1995) *J. Biol. Chem.* 270, 6856–6863.
- [5] Arkin, I.T., Russ, W.P., Lebendiker, M. and Schuldiner, S. (1996) *Biochemistry* 35, 7233–7238.
- [6] Schwaiger, M., Lebendiker, M., Yerushalmi, H., Coles, M., Groeger, A., Schwarz, C., Schuldiner, S. and Kessler, H. (1998) *Eur. J. Biochem.* 254, 610–619.
- [7] Yerushalmi, H., Lebendiker, M. and Schuldiner, S. (1996) *J. Biol. Chem.* 271, 31044–31048.
- [8] Steiner Mordoch, S., Granot, D., Lebendiker, M. and Schuldiner, S. (1999) *J. Biol. Chem.* 274, 19480–19486.
- [9] Muth, T.R. and Schuldiner, S. (2000) *EMBO J.* 19, 234–240.
- [10] Torres, J. and Arkin, I.T. (2000) *Eur. Biochem. J.*, in press.
- [11] Gottschalk, K., Schuldiner, S., Kessler, H. (2000) *J. Mol. Biol.*, submitted.
- [12] Smith, S.O., Aschheim, K. and Groesbeek, M. (1996) *Q. Rev. Biophys.* 29, 395–449.
- [13] Opella, S.J. (1997) *Nature Struct. Biol.* 4, 845–848.
- [14] Watts, A., Burnett, I.J., Glaubitz, C., Grobner, G., Middleton, D.A., Spooner, P.J.R. and Williamson, P.T.F. (1998) *Eur. Biophys. J.* 28, 84–90.
- [15] Spooner, P.J.R., Rutherford, N., Watts, A. and Henderson, P.J.F. (1994) *Proc. Natl. Acad. Sci. USA* 91, 3877–3881.
- [16] Mehring, M. (1983) *Principles of High Resolution NMR in Solids*, Springer Verlag, Berlin.
- [17] Middleton, D.A., Robins, R., Feng, X.L., Levitt, M.H., Spiers, I.D., Schwalbe, C.H., Reid, D.G. and Watts, A. (1997) *FEBS Lett.* 410, 269–274.
- [18] Williamson, P.T.F., Gröbner, G., Miller, K. and Watts, A. (1998) *Biochemistry* 37, 10854–10859.
- [19] Demco, D.L., Tegenfeldt, J. and Waugh, J.S. (1975) *Phys. Rev. B* 11, 4133–4151.
- [20] Schaefer, J., Stejskal, E.O. and Buchdahl, H. (1977) *Macromolecules* 10, 384–405.
- [21] Stejskal, E.O., Schaefer, J. and McKay, R.A. (1984) *J. Magn. Reson.* 57, 471–485.
- [22] Grim, S.O., McFarlane, W., Davidoff, E.F. and Marks, T.J. (1966) *J. Phys. Chem.* 70, 581–585.
- [23] Stohrer, J., Gröbner, G., Reimer, D., Weisz, K., Mayer, C. and Kothe, G. (1991) *J. Chem. Phys.* 95, 672–678.
- [24] Weisz, K., Gröbner, G., Mayer, C., Stohrer, J. and Kothe, G. (1992) *Biochemistry* 31, 1100–1112.
- [25] Van Wazer, J.R. and Letcher, L.H. (1967) in: $^{31}\text{P-NMR}$ (Crutchfield, M.M., Dungan, C.H. and Letcher, L.H., Eds.), pp. 75–225, Wiley Interscience, New York.
- [26] Ahmed, M., Borsch, C.K., Taylor, S.S., Vazquez-Laslop, N. and Neyfakh, A.A. (1994) *J. Biol. Chem.* 269, 28506–28513.
- [27] Zheleznova, E.E., Markham, P.N., Neyfakh, A.A. and Brennan, R.G. (1999) *Cell* 96, 353–362.
- [28] Gorenstein, D.G. (1984) in: $^{31}\text{P-NMR}$ (Gorenstein, D.G., Ed.), pp. 7–36, Academic Press, New York.
- [29] Nageswara Rao, B.D. (1984) in: $^{31}\text{P-NMR}$ (Gorenstein, D.G., Ed.), pp. 57–103, Academic Press, New York.
- [30] Bock, J.L. and Sheard, B. (1975) *Biochem. Biophys. Res. Commun.* 66, 24–30.
- [31] Chlebowski, J.F., Armitage, I.M., Tuas, P.P. and Coleman, J.E. (1976) *J. Biol. Chem.* 254, 1207–1216.
- [32] Hull, W.E., Halford, S.E., Gutfreund, H. and Sykes, B.D. (1976) *Biochemistry* 15, 1547–1561.
- [33] Yerushalmi, H. and Schuldiner, S. (2000) *J. Biol. Chem.* 275, 5264–5269.
- [34] Yerushalmi, H., Steiner-Mordoch, S. and Schuldiner, S. (2000), in preparation.